JOURNAL OF MATERIALS SCIENCE 27 (1992) 6695–6699

X-ray topographic observation on the annealing process of pure iron crystal

A. MIHARA, Y. TANEDA
Department of Mathematics and Physics, National Defence Academy, Yokosuka 239, Japan

The annealing process of a thin crystal of zone-refined pure iron has been investigated using X-ray transmission topography. Dislocation structures of (1 0 0) crystal were successively observed after annealing at 630, 780 and 840 °C. The dislocation density was about 5×10^3 cm^{-2} after annealing at 780 °C, and 5×10^2 cm^{-2} after annealing at 840 °C. The Burgers vector of the dislocation resolved individually was $a/2\langle 1\,1\,1\rangle$. The dislocation line became straight and short, and lay on the $\{1\,1\,0\}$ plane after annealing.

1. Introduction

X-ray transmission topography is very useful technique to investigate the dislocation structure in nearly perfect crystals. Nevertheless, this technique has been rarely applied to pure iron crystals because of their great imperfections, with the exception of iron whiskers [1–4]. In the previous paper [5], 90° magnetic domain wall arrangements in zone-refined pure iron crystals were studied by this technique.

The purposes of the present work were to investigate the annealing process of pure iron thin crystals and to elucidate the annihilation behaviour of the dislocation structure on annealing, by X-ray transmission topography.

2. Experimental procedure

A pure iron crystal with (1 0 0) face was prepared [5] in the following way. An iron rod, 10 mm diameter, was zone-refined by six passes in a dry hydrogen atmosphere and two in wet hydrogen using horizontal induction zone-melting. The purified part ($R_{300}/R_{4.2} = 300$) was cold-rolled to 0.25 mm thickness, then thinned 0.21 mm by chemical polishing. The plate was heated at 880 °C for 11 h in a dry hydrogen atmosphere, and was then cooled to room temperature at a rate of 100 °C h^{-1}. A (1 0 0) crystal plate was carefully polished chemically to 70 μm thickness. X-ray topographs were taken with reflection from four $\{1\,1\,0\}$ planes and four $\{2\,0\,0\}$ planes normal to the crystal surface, with Lang's method using AgK_{α_1}, where μt was 1.1. To observe the annealing behaviour of dislocation structures in the crystal, the topographs were successively taken after (1) chemical polishing, (2) annealing at 630 °C for 3 h, (3) annealing at 780 °C for 2 h, and (4) annealing at 840 °C for 1 h. The heating and cooling rates were 100 °C h^{-1} on each annealing. All the topographs are shown with negative contrast; i.e. dark regions on the topograph correspond to regions of large X-ray intensity. In general, crystal defects such as dislocations are shown as black images.

3. Results

Fig. 1 shows a series of X-ray transmission topographs of the annealing process of zone-refined pure iron crystals. Fig. 1a was obtained after chemical polishing. Two white regions, one circular and the other narrow in shape, are the included grains, because the grains do not satisfy the Bragg condition. The black regions, about half of the entire field, are due to existing grown-in dislocations with very high density. In the other regions, 90° magnetic domain wall images are indistinctly observed. Fig. 1b was obtained after annealing at 630 °C for 3 h. The included grain, seen as a circular shape, completely vanished, and also the black regions almost disappeared, indicating that grain growth occurs, and that the crystal becomes more perfect during 630 °C annealing. Rearrangements of the magnetic domain structure and the dislocation structure are observed in Fig. 1c, which was obtained after annealing at 780 °C, a temperature just above the Curie point (T_c = 769 °C). A topograph of the same region is shown in Fig. 1d after additional annealing at 840 °C for 1 h.

Fig. 2 is a $0\,0\,\bar{2}$ topograph after annealing at 780 °C for 2 h, in which are seen subgrain boundaries and dislocation clusters in addition to many magnetic domain walls. The distribution of dislocations in the crystal is of uneven density; in the upper region of the topograph, dislocation density is low, about 2×10^3 cm^{-2}, and in the lower region it is high, 7×10^3 cm^{-2}.

Fig. 3a–c are 0 2 0, $0\,1\,\bar{1}$ and 0 1 1 topographs, respectively, taken from the same region as the upper part of Fig. 1. The 90° magnetic walls, closure domains (fir-tree branches), the black-white image and the $\langle 0\,0\,1\rangle$ image [5] are seen on the topographs. In Fig. 3b and c, the images of fir-tree branches and 90° magnetic domain walls normal to the reflection vector are invisible, according to the invisibility criterion for $\{1\,1\,0\}$ 90° magnetic domain wall. The $\langle 0\,0\,1\rangle$ images as seen in Fig. 3b and c, several tens of micrometres in width, were frequently observed with respect to the magnetic domain configuration. These images are still

0022–2461

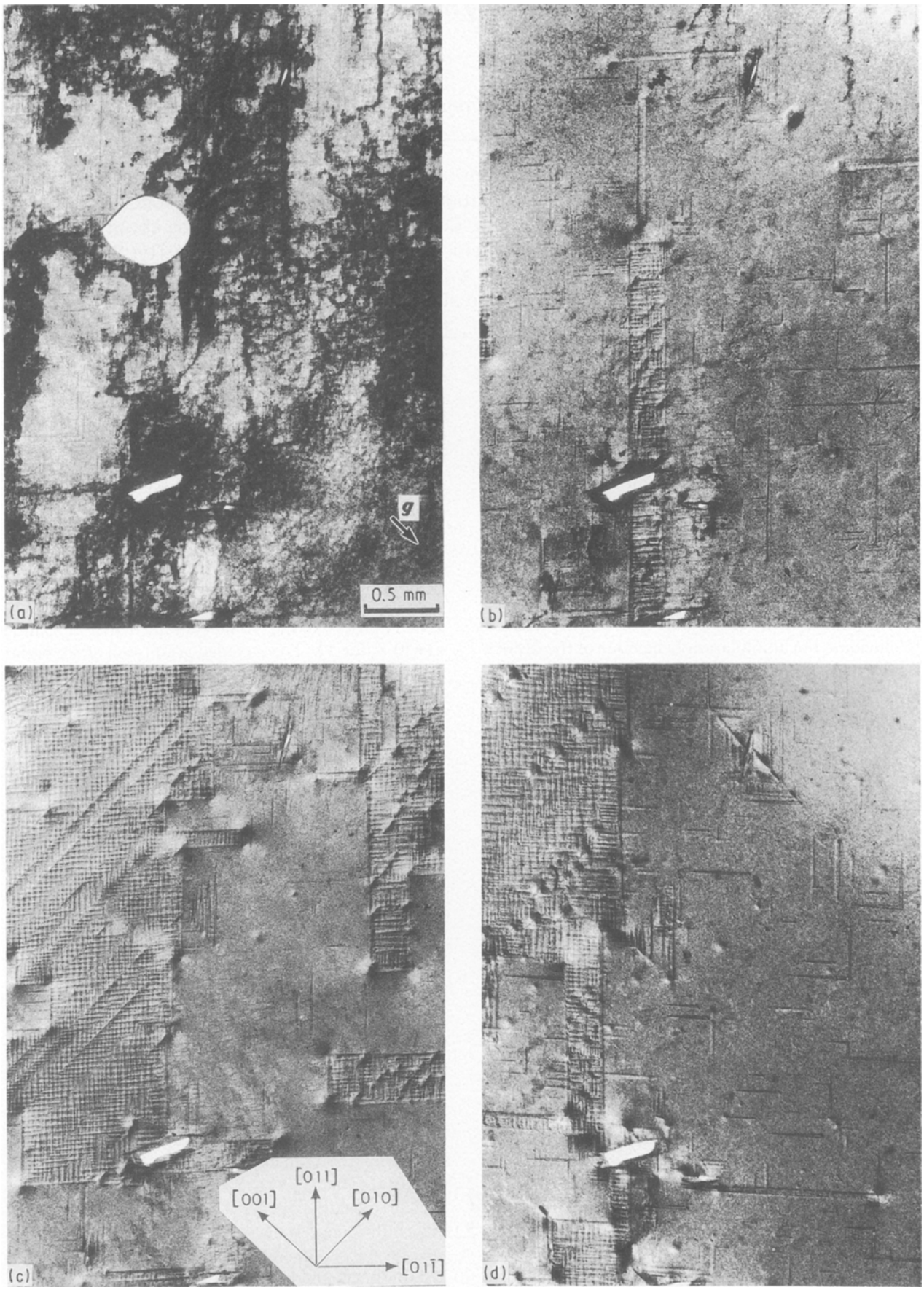

Figure 1 X-ray topographs showing the annealing (in a hydrogen atmosphere) sequence of pure iron crystals. (a) after chemical polishing, (b) after annealing at 630 °C for 3 h, (c) after annealing at 780 °C for 2 h, and (d) after annealing at 840 °C for 1 h. (a–c) 0 2 0 reflection, (d) 0 0 2 reflection.

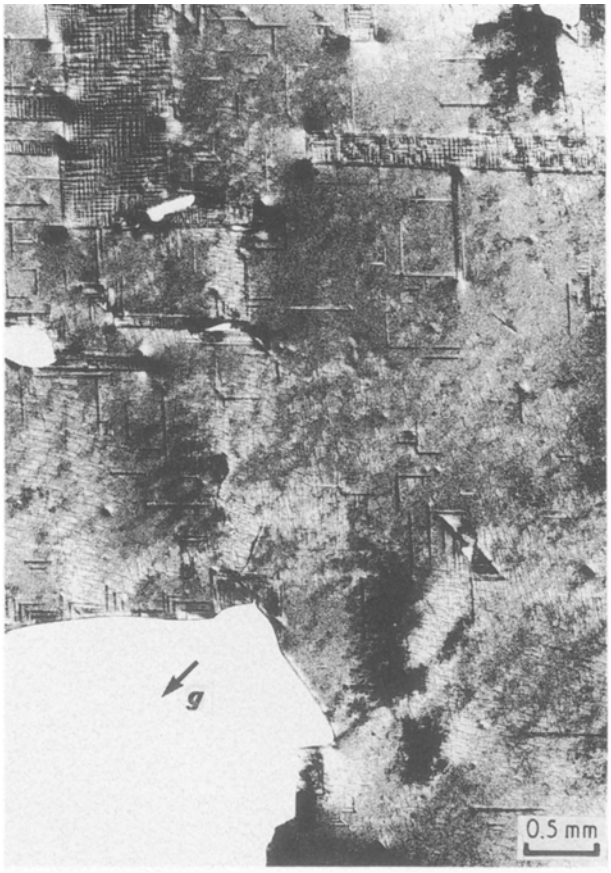

Figure 2 A $00\bar{2}$ topograph showing the dislocation structure after annealing at 780 °C for 2 h.

not visible in Fig. 3a, and have not yet been perfectly explained. The dislocations to the left in the topograph are visible in Fig. 3a and b, but are invisible in Fig. 3c. Therefore, these dislocations should have a Burgers vector of $a/2[1\,\bar{1}\,1]$ or $a/2[1\,1\,\bar{1}]$, according to the invisibility criterion of the dislocation image. Fig. 4a and b are topographs of the same region taken after annealing at 780 °C for 2 h and at 840 °C for 1 h, respectively. In Fig. 4a, the dislocation line seems to lie, for the most part, roughly along $[0\,1\,1]$ or $[0\,\bar{1}\,1]$ directions, and the dislocation density is about 7×10^3 cm^{-2}, but the dislocation density estimated in Fig. 4b is about 5×10^2 cm^{-2}. Furthermore, the dislocations as seen in Fig. 4b are very short, nearly equal to two or three times the thickness of specimen in length, and are straight, more exactly in two $\{0\,1\,1\}$ directions. Thus it is difficult to distinguish between the dislocation image and the wall image.

A distinction between the dislocations and the 90° magnetic domain walls may be seen in Fig. 5a and b, where the reflection vectors are $[0\,0\,2]$ in the former and $[0\,\bar{1}\,1]$ in the later. In Fig. 5b, wall images parallel to the reflection vector appeared according to the invisibility criterion. However, many dislocation images parallel to the reflection vector have disappeared in this topograph. Consequently, these dislocations

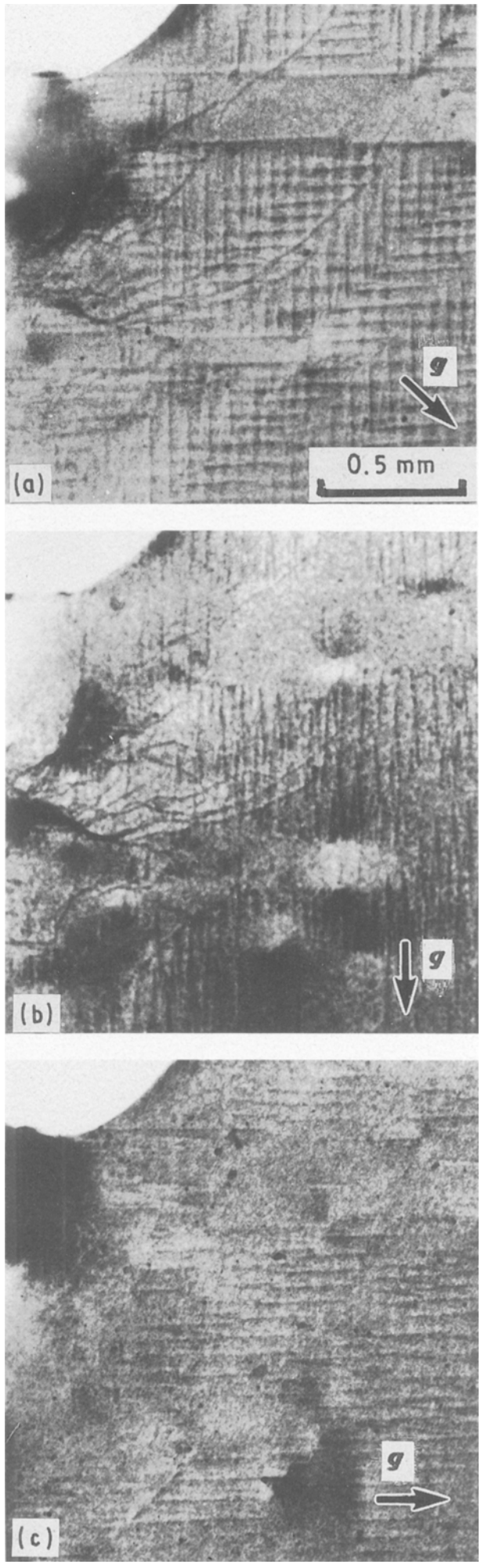

Figure 3 X-ray topographs showing visibility condition for the dislocation after 780 °C annealing. (a) 020, (b) $01\bar{1}$ and (c) 011 reflection.

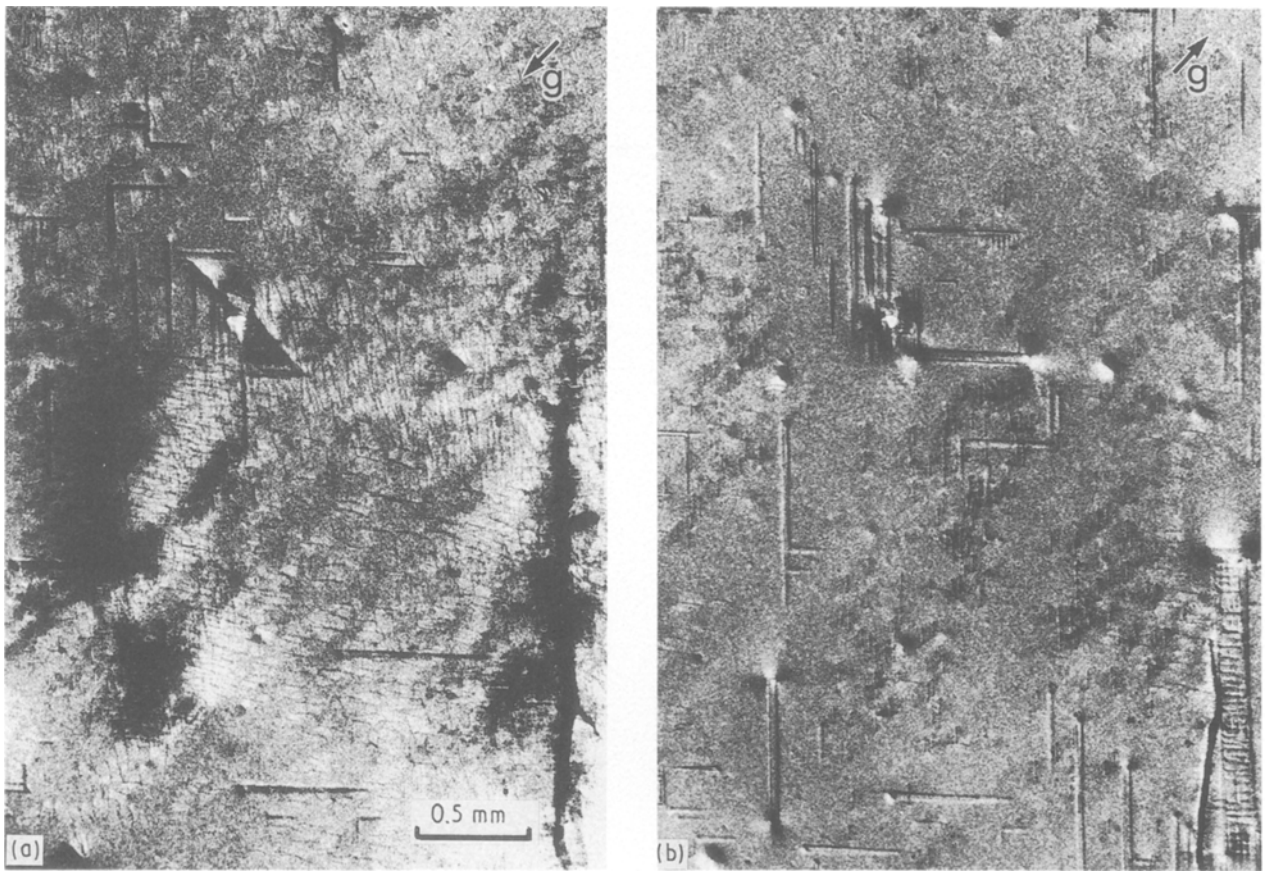

Figure 4 Topographs showing a transformation of the dislocation structure after annealing at 840 °C for 1 h. (a) 0 0 $\bar{2}$ and (b) 0 0 2 reflection.

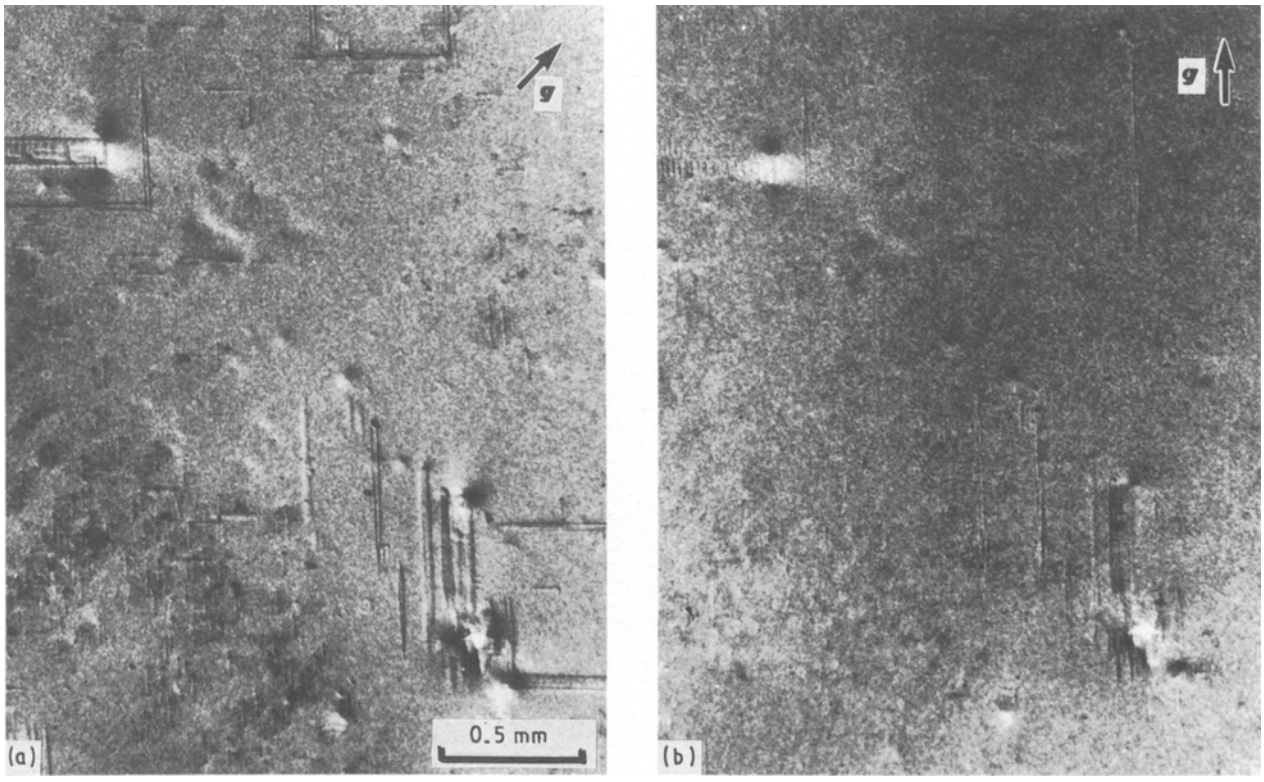

Figure 5 Topographs showing visibility condition for the dislocation after 840 °C annealing. (a) 0 0 2 and (b) 0 $\bar{1}$ 1 reflection.

should have a Burgers vector of $a/2[1\,1\,1]$ or $a/2[1\,\bar{1}\,\bar{1}]$, lying on the $\{0\,1\,1\}$ plane, and perhaps running through specimen from one surface to the other. These dislocation images show a marked modulation of intensity along their length in the 0 0 2 reflection, as seen in Fig. 5a [6].

4. Discussion

As the as-grown crystal was polished chemically from 0.21 mm to 70 μm thick, Fig. 1a shows the dislocation structure in the middle part of the thickness in an as-grown crystal. In this figure, large cell structures and tangled dislocation clusters are observed to have a

very high dislocation density. However, the dislocation density rapidly decreased as the annealing temperature was lowered below 880 °C: it is 5×10^3 cm^{-2} after annealing at 780 °C for 2 h, and 5×10^2 cm^{-2} after annealing at 840 °C for 1 h. Some dislocation annihilation may occur by a dislocation dipole mechanism, but the major part is considered to occur by dislocations escaping from the crystal surface.

Let us suppose that the crystal consists of a region with low dislocation density in the neighbourhood of the crystal surface, and a region with high dislocation density in the middle part of the crystal thickness. A difference in free energy, F, between the two regions will create a driving force. The migration rate of dislocations in the region with high dislocation density is in proportion to $F \exp(-U/kT)$, where U is the activation energy to overcome the other dislocation, k Boltzmann's constant, and T the annealing temperature. When the crystal is very thin, the dislocations acting as an obstacle will escape from the crystal surface, and immediately decrease with annealing. The region with low dislocation density will also spread out immediately; U also will immediately become zero. However, when the crystal is thick, a transition region will be formed between the two regions, and will intercept the migration of dislocations in the region having high dislocation density and then the dislocations will cease to escape from the crystal surface. The critical thickness between thin and thick crystals is about 90 μm in this experiment, which perhaps depends on the purity of the crystal.

References

1. Y. CHIKAURA, *Jpn J. Appl. Phys.* **15** (1976) 385.
2. Y. CHIKAURA and B. K. TANNER, *ibid.* **18** (1979) 1389.
3. S. NAGAKURA and Y. CHIKAURA, *J. Phys. Soc. Jpn* **30** (1971) 495.
4. Y. CHIKAURA and S. NAGAKURA, *Jpn J. Appl. Phys.* **11** (1972) 158.
5. T. YAMASHITA and A. MIHARA, *ibid.* **10** (1971) 1661.
6. A. R. LANG and M. POLCAROVÁ, *Proc. Roy. Soc.* **A285** (1965) 297.

Received 2 September 1991
and accepted 7 May 1992